Int J Earth Sci (Geol Rundsch) (2001) 90:484–499
DOI 10.1007/s005310100174

ORIGINAL PAPER

F. Schlunegger · J. Melzer · G.E. Tucker

Climate, exposed source-rock lithologies, crustal uplift and surface erosion: a theoretical analysis calibrated with data from the Alps/North Alpine Foreland Basin system

Received: 21 March 2000 / Accepted: 4 November 2000 / Published online: 2 June 2001

Abstract Paleofloristic data imply that paleoclimate changed in the Swiss Alps at the Oligocene/Miocene boundary from humid and hot conditions toward a climate with high temperature and low humidity. The aridization is associated with a change in depositional pattern from alluvial fans to lakes and floodplains, suggesting decreasing sediment discharge. A further 25–40% decrease of sediment discharge occurred at ca. 20 Ma when the orogenic core of the Alps became exposed to the surface. We applied a surface processes model to explore potential controls on the pattern of sediment discharge and on the evolution of the Alpine drainage basin. The model is based on the presumption that the rates of fluvial incision into bedrock are proportional to shear-stress exerted by the flowing water. The model results imply that the paleoclimate change resulted in an instantaneous decrease of sediment discharge and a vertical topographic growth until steady-state conditions between erosional and crustal mass flux are established. However, exposure of the crystalline core of the Alps at ca. 20 Ma is likely to have resulted in the 25–40% decrease of sediment discharge and the reorganization of the drainage pattern from an orogen-normal to an orogen-parallel orientation of dispersion.

Keywords Surface processes model · Paleotopography · Denudation · Surface erosion · Source rocks and erosion

F. Schlunegger (✉) · J. Melzer
Institut für Geowissenschaften, Friedrich-Schiller-Universität, Burgweg 11, 07749 Jena, Germany

G.E. Tucker
University Lecturer in Geocomputation and Fellow of Brasenose College, School of Geography and the Environment, Oxford University, Mansfield Road, Oxford OX1 3TI3, UK

Present address:
F. Schlunegger, Dept. of Earth Sciences. ETHZ, Sonneggstr. 5, CH-8092 Zürich, Switzerland
e-mail: fritz.schlunegger@erdw.ethz.ch

Introduction

The drainage pattern of the Swiss Alps evolved from an orogen-normal to the present-day orogen-parallel orientation (Rhein and Rhone valleys; Fig. 1), at a time when the Alps are considered to have experienced a phase of constructive growth (Schlunegger 1999). However, despite the formation of enhanced relief, the volume of sediment preserved in the stratigraphy of the North Alpine Foreland Basin (NAFB) suggests that there was a significant decrease in the discharge of sediment from the Central Alps at ca. 20 Ma compared with the preceeding 10 My (Schlunegger 1999; Kuhlemann et al. 2000).

The aim of this paper is to explore possible controls on the Early Miocene decrease of surface erosion rates in the Central Alps. Also, we formulate hypotheses for why the drainage pattern changed from an orogen normal to an orogen-parallel orientation as is observed presently (Rhone and Rhein valleys; Fig. 1). The parameters that are considered are changes in rates and pattern of crustal uplift, exposed source-rock lithologies and paleoclimate (e.g., Whipple and Tucker 1999; Kühni and Piffner, in press). In a first step of our analysis, we present a synthesis of the geodynamic evolution of the Central Alps including the structural development of the orogen, the geometric evolution of the Alpine drainage basin, and estimated variations in surface erosion rates or discharge of sediment to the NAFB. Furthermore, data regarding temporal and spatial variations in exposed source-rock lithologies and paleoclimate (both of which influence surface erosion) are extracted from published data on the petrographic evolution of the deposits in the NAFB, and from paleobotanic data of temporally calibrated fossil sites. In the final step of our analy-

Fig. 1 **A** Geological map of the Central Swiss Alps and large-scale stratigraphy of the Molasse Basin which borders the Alps to the north. *I, II, III* Deposits of the Speer-Hörnli, Rigi-Höhronen and Honegg-Napf palaeorivers; *AR* Aiguille Rouge massif; *Mo* Mont Blanc massif; *Aar* Aar massif; *Go* Gotthard nappe. **B** Tectonic section across the Central Alps of eastern Switzerland and northeastern Italy. *NAFB* North Alpine Foreland Basin. (Modified after Schmid et al. 1996) ▶

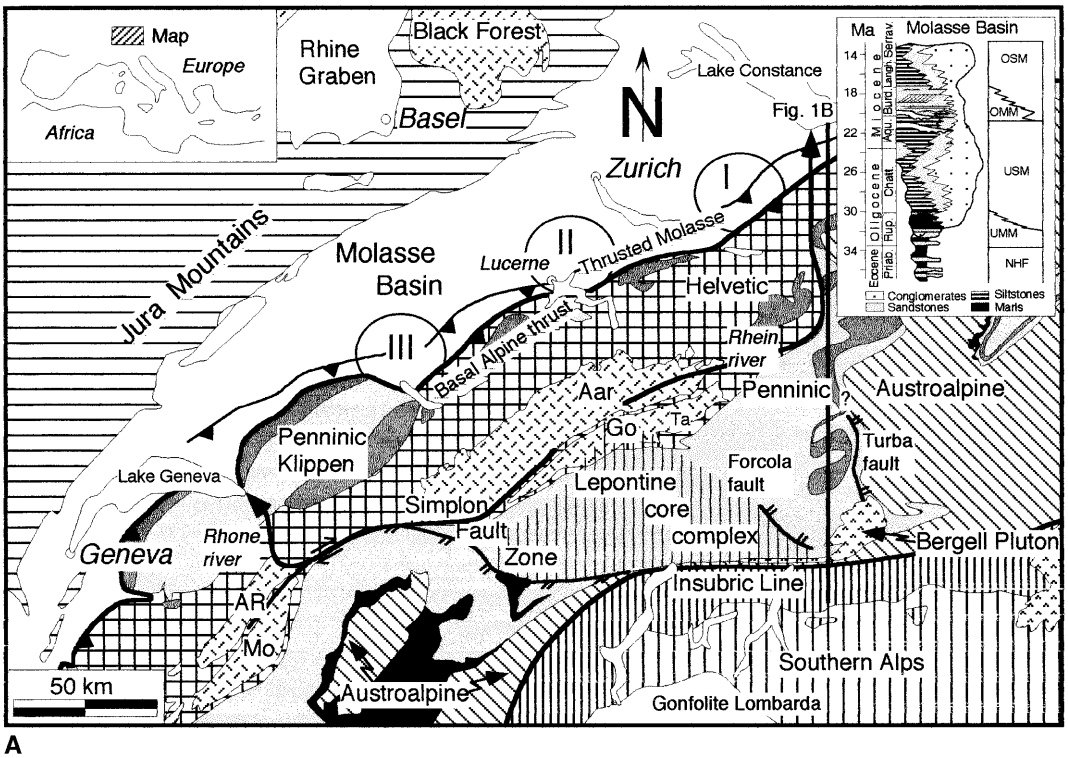

A

- Autochthonous sedimentary cover of the north European foreland plate
- Penninic thrust nappes (Prealps and crystalline nappes)
- Penninic and Ultrahelvetic flysch
- Helvetic thrust nappes
- Basement uplift of the north European foreland plate
- Lepontine dome (area that experienced tectonic exhumation)
- Ophiolites
- Austroalpine thrust nappes
- Sedimentary cover of Southern Alps
- Crystalline core of Southern Alps
- Tertiary plutons

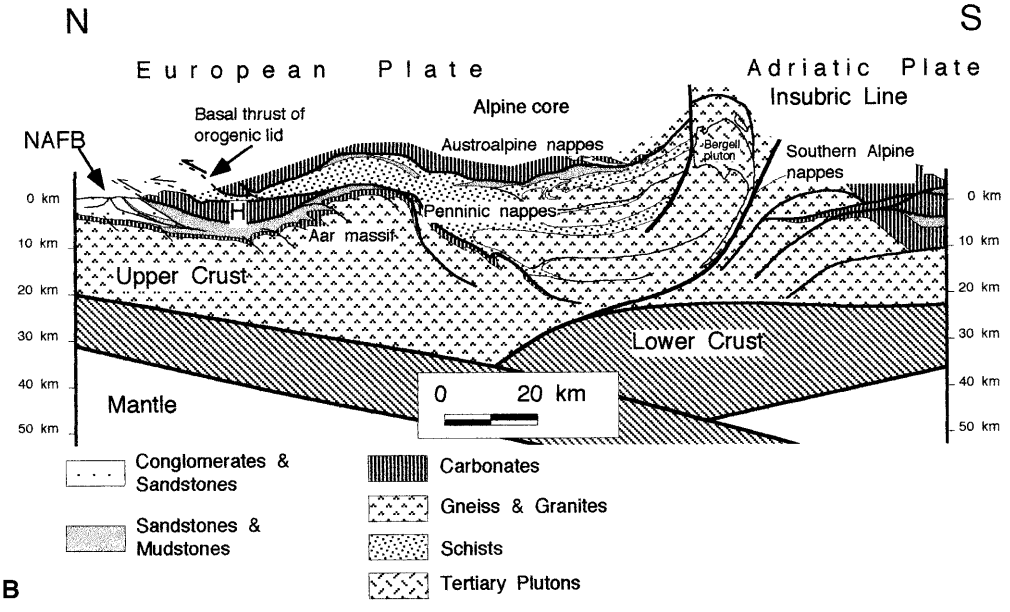

B

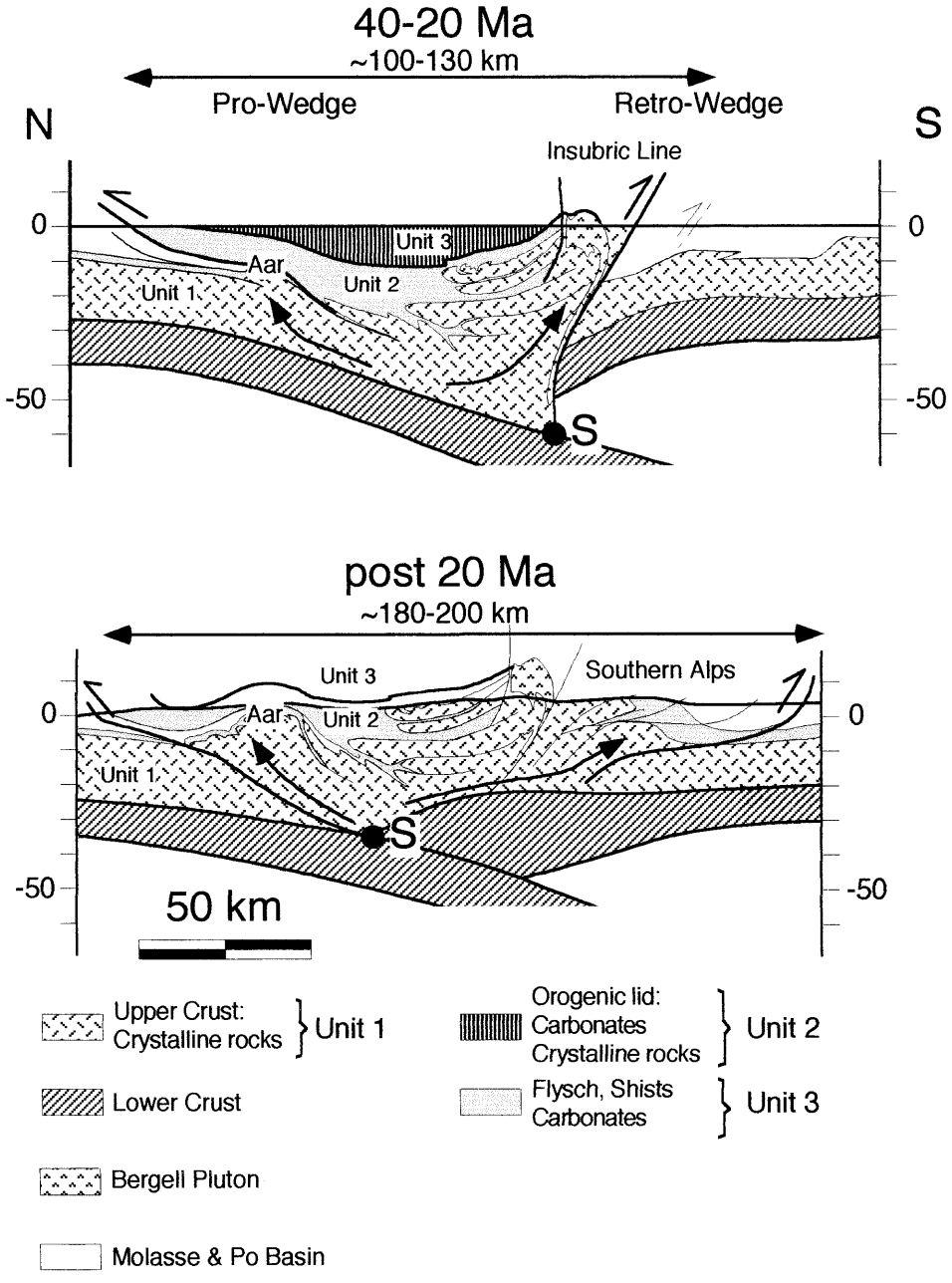

Fig. 2 The evolutionary steps of the Central Alps and the litho-tectonic architecture. *S* Singularity, location where the upper crust was detached from the lower crust. (Modified after Schmid et al. 1996)

sis, we examine the potential role of (a) climate change and (b) variations in exposed source-rock lithologies on surface erosion rates by applying a surface processes model which is based on the shear stress formulation for fluvial erosion. Model boundary conditions and constraints on model input parameters are provided by the structural data from the orogen, and by information on sediment discharge, exposed source-rock lithologies, and paleoclimate.

Geologic setting

The Alps: lithologic architecture and structural evolution

The present-day Alps (Fig. 1) consist of upper crustal material in the orogenic core, and thick-skinned and thin-skinned thrust sheets on the external flanks (Schmid et al. 1996). The crystalline basement is part of the upper European and African continental crust (unit I in Fig. 2). It consists of highly metamorphosed crystalline lithologies which are exposed in the core of the Alps (Penninic crystalline nappes), and of low-grade metamorphosed crystalline rocks which crop out in the external massifs (e.g., Aar massif; Figs. 1, 2) and in the Southern Alpine nappes. In the north, these units are structurally overlain by the 500-m to several-kilometres-thick piggy-back stack of north-vergent Penninic sedimentary and Helvetic thrust nappes (unit 2 in Fig. 2). The deposits of these nappes consist of deep marine sandstones and shales (Bündner schists), or shallow marine carbonates and shales (Helvetic thrust nappes and

Penninic Klippen; Fig. 1). Unit 2 also comprises siliciclastic sedimentary rocks which accumulated in subbasins on the European foreland plate (Penninic and Ultrahelvetic/Helvetic flysch nappes) as continent–continent collision proceeded (Lihou and Allen 1996). Helvetic and Penninic thrust sheets are overlain by the Austroalpine nappes that form the orogenic lid (unit 3 on Fig. 2). This unit consits of crystalline rocks and carbonates (Fig. 1B) of the Apulian promontory of the African plate. In the south, the Penninc and Austroalpine nappes are separated from the south-vergent Southern Alpine nappes by the E/W-striking Insubric Line. This suture accommodated the late stage of collision between the Central Alps and the Adriatic promontory by steep S-directed backthrusting and right-lateral strike-slip movement.

According to coupled erosion-thermomechanical models for the evolution of the Swiss Alps, Schlunegger and Willett (1999) thought that this orogen experienced two stages of orogenesis (Fig. 2). During the first stage, between ca. 40 and 20 Ma (Fig. 2A), the Alps are considered to have adapted a distinct geometry with a low-tapered pro-wedge facing the vergence of subduction, and a high-tapered retro-wedge on the opposite side. The retro-wedge was separated from its retro foreland (South Alpine Foreland Basin, SAFB) by a shear zone (Insubric Line) along which backthrusting at rates of >1 km/My occurred (Schmid et al. 1996). This backthrust was rooted in the location where the lower crust of the subducting European plate was decoupled from the upper crust (singularity; Fig. 2A). Accretion of upper crustal material at the tip on the pro-side of the Alpine wedge (deformation of the Penninic and Helvetic thrust nappes; Schmid et al. 1996) presumably kept the taper at an at-yield mechanical stage. Starting at ca. 25 Ma, a phase of enhanced tectonic extension that occurred by southwestward directed slip along the Simplon Fault Zone resulted in a considerable amount of exhumation (Fig. 1; Steck and Hunziker 1994). In the Early Miocene (stage II), the outward growth of the Alps (deformation of the Southern Alps and Jura Mountains, (Fig. 2B) implies a constructive phase of orogen growth (Schlunegger 1999) consistent with low exhumation rate relative to the rate of crustal accretion (stage II; Schlunegger and Willett 1999). The age of deformation especially of the Southern Alps is constrained at ca. 18 Ma by cross-cutting relationships between temporally calibrated sediments and structures (Schmid et al. 1996). At approximately the same time, rates of accretion of upper crustal material on the pro-side of the Alps were enhanced (deformation of the Aar massif; Fig. 1), resulting in surface uplift and re-routing of Alpine paleorivers (Schlunegger 1999).

Stratigraphic architecture of the NAFB

The peripheral North Alpine Foreland Basin (NAFB), located north of the Alps, provides the most important information for reconstructing the erosional history of the Swiss Alps. The large-scale stratigraphic development of this basin is considered to reflect an early underfilled and a later overfilled stage of basin evolution which is referred to as Flysch and Molasse in classic Alpine literature (Sinclair and Allen 1992). The Molasse deposits that accumulated between the Early Oligocene and the Middle Miocene (Fig. 1; Kempf et al. 1998) comprise two coarsening- and thickening-upward megasequences (Matter et al. 1980). The first megasequence starts with construction of the 35- to 30-Ma-old Lower Marine Molasse Group (UMM). This unit forms the transition from the underfilled to the overfilled stage of basin evolution presumably as the increase of sediment supply rates (Kuhlemann et al. 2000) was larger than that of accommodation space creation. The UMM is overlain by the fluvial clastics of the 30- to 20-Ma-old Lower Freshwater Molasse Group (USM). This unit consists of several kilometres of alluvial fan conglomerates which were constructed at the Alpine thrust front (e.g., Kempf et al. 1999). Toward more distal sites of the basin, the conglomerates interfinger with meander belt sandstones, floodplain mudstones, and lacustrine depositional systems (Platt and Keller 1992).

Construction of the second megasequence started with a marine transgression at ca. 20 Ma (Keller 1989), resulting in establishment of the shallow marine depositional systems of the Upper Marine Molasse Group (OMM) between 20 and 16.5 Ma (Kempf et al. 1998). At the Alpine thrust front, the marine deposits interfinger with fan delta conglomerates which were sourced in the Central Alps (Keller 1989). A second source of elastic material was located in the Bohemian massif approximately 100 km northeast of the study area, from where sediment was imported by strong tidal currents (Allen et al. 1985). The OMM is overlain by the continental Upper Freshwater Molasse Group (OSM). Deposition of the OSM started at ca. 16.5 Ma. The youngest deposits of this unit display ages of between 13 Ma (proximal position; Kempf et al. 1999) and 10.5 Ma (distal position; Berger 1992). At present, the Molasse Basin is uplifted and eroded, and no deposits younger than Tortonian are found.

Denudation of the Central Alps

Evolution of Alpine drainage pattern

We use the most recent reconstruction of the evolution of the drainage pattern of the Swiss Alps presented by Schlunegger et al. (1998) and subsequently modified by Eynatten et al. (1999). The reconstruction of these authors is based on (a) detailed provenance analyses of key clasts deposited in the foreland basins (e.g., Matter 1964; Gasser 1968; Stürm 1973), and (b) determination of the thermo-chronometric evolution of detrital mica and zircon/apatite crystals which is then compared with the pattern of cooling in the hinterland (Giger 1991; Eynatten et al. 1999). These data resulted in identification of two stages of drainage pattern evolution

(Schlunegger et al. 1998; Eynatten et al. 1999). During the first stage, between the Late Oligocene and the Early Miocene, the Alpine drainage system is considered to have displayed an orogen-normal pattern with a drainage divide that was located in the rear of the wedge approximately 20–40 km north of the Insubric Line (Fig. 3A). The second phase of drainage basin evolution is considered to have been initiated in the Early Miocene (Schlunegger et al. 1998). It is characterized by development of an orogen-parallel drainage pattern with sources in the Central Alps (Fig. 3B). This modification in the organization of the Alpine drainage basin appears to have occurred as Alpine paleorivers were rerouted around the hinge of the growing Aar massif. Specifically, at ca. 21 Ma, alluvial fan construction in Central Switzerland (Rigi-Höhronen alluvial fan, Luzern area; Fig. 1A) stopped. Key clasts of this palaeoriver (red granites) are identified in the alluvial fan conglomerates approximately 50–70 km farther east (Speer-Hörnli paleoriver). We show that exposure of the highly erodible unit 2 in the Early Miocene is sufficient to cause the reorganization of the drainage pattern.

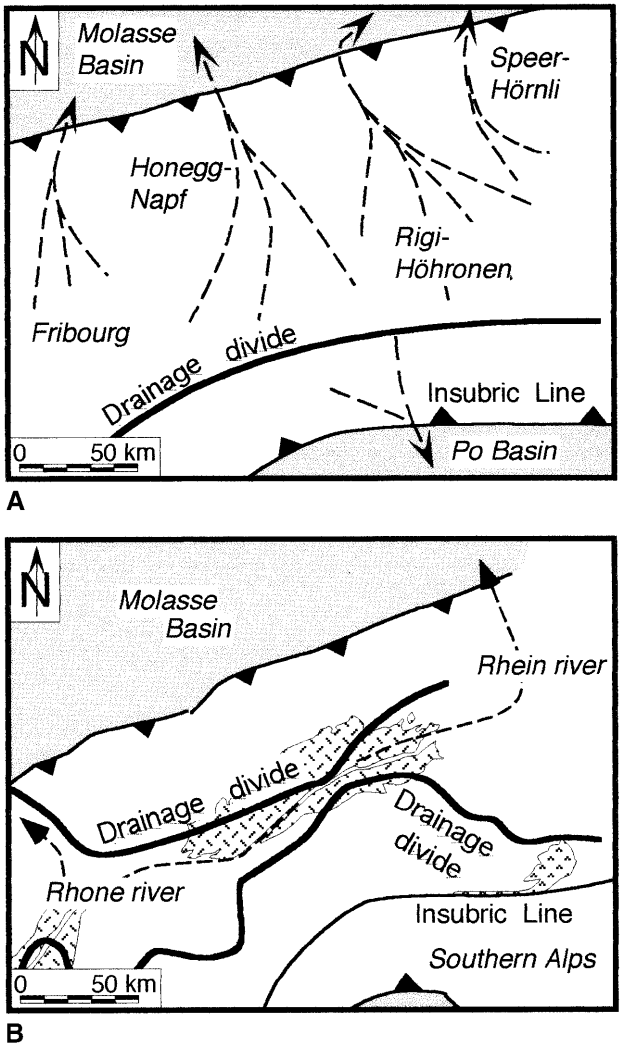

Fig. 3 The drainage pattern of the Central Alps during **A** the Late Oligocene and **B** at present. (Modified after Schlunegger et al. 1998)

Surface erosion rates

Information to reconstruct temporal variations of surface erosion rates is provided by the volume of deposited rocks per unit time that can be converted into sediment discharge (see Kuhlemann et al. 2000 for discussion of methodology). In this paper we present the sediment budget analysis of Hay et al. (1992), of Schlunegger (1999; Tables 1, 2, 3), and of Kuhlemann et al. (2000). We simply present the data of these authors for the sake of completeness, but we do not intend to comment on the differences between the results.

Export and import of sediment into sedimentary basins has to be discussed carefully because the basin was laterally open. During USM time (30–20 Ma) a significant amount of sediment was exported to the NE to the German part of the basin by strong axial sediment transport (Berger 1992). This implies that determinations of sediment discharge to the Swiss part of the NAFB (e.g., Schlunegger 1999) represent an underestimate. For the OMM situation, tidal circulation modeling (Martel et al. 1994) and delineation of petrographic provinces and

Table 1 Stratigraphic data of the Molasse Basin. A compilation and discussion of the data in terms of temporal resolution is presented by Schlunegger (1999). Additional data is taken from Kempf et al. (1999) for the Hörnli, Necker and Steintal sections, and from Kempf and Matter (1999) for the Zürich section. The location of the wells and the sections is presented in Fig. 4A

Well/section	Compacted thicknesses (m)			
	30–25 Ma	25–20 Ma	20–16.5 Ma	16.5–3.5 Ma
Tschugg-1	250	>250	–	–
Ruppoldsried-1	400	>500	–	–
Linden-1	1600	1600	1000	–
Thun-1	2150	1950	–	–
Althishofen-1	120	800	>300	–
Entlebuch-1	500	2100	–	–
Emme	1200	–	–	–
Honegg	1500	–	–	–
Schafisheim	0	>250	–	–
Boswil-1	350	720	460	–
Hünenberg-1	450	1140	990	–
Rigi	3600	–	–	–
Einsiedeln	2700	–	–	–
Necker	1950	2050	–	–
Steintal	1700	–	–	–
Berlingen-1	0	700	200	–
Kreuzlingen-1	0	1000	200	–
Lindau-1	0	1050	300	–
Künsnacht-1	0	1500	550	–
Brochene Fluh	0	100?	–	–
Höhronen	–	2000	–	–
Napf	–	–	1050	850
Hörnli	–	–	1000	650
Zürich	–	–	–	600

Table 2 Preserved volumes of sediment and estimation of average erosion rates

Time interval (Ma)	Deposited volume of sediment (km^3)	Size of drainage basin (km^2)	Erosion rates (m/My)
30–25	13,000	12,000	200±100
25–20	15,000	12,000	250±125
20–16.5	3500	12,000	85±40
16.5–13.5	3300	12,000	90±45

Part of this compilation has already been published by Schlunegger (1999). Here we simply expand the data set of this author to eastern Switzerland to incorporate the whole magneto-stratigraphic data set of the Swiss Molasse (Kempf et al. 1998, 1999). The size of the drainage basin is based on estimates from Fig. 3A

Table 3 Volumetric mass balance calculations of sediment derived from the Central Alps after Hay et al. (1992). For the Late Oligocene, we considered the Swiss Molasse Basin, the German Molasse Basin and the Rhein Graben as sinks for the sediment derived from the Central Alps (Berger 1996). For the Early and the early Middle Miocene we considered the data from the Swiss and German Molasse Basins (e.g., Allen et al. 1985; Berger 1996), and for later time intervals we also included the sediments in the Rhone Delta/Gulf of Lion as well as in the Rhone and Bresse Grabens (Hay et al. 1992). The recalibration of the regional stages is taken from Kempf et al. (1998). Conversion of load (Hay et al. 1992) to volume is based on an average density of 2.4 g/cm^3

Time interval (Ma)	Deposited volume of sediment (km^3)	Size of drainage basin (km^2)	Erosion rates (m/My)
34–30	2000	12,000	40±20
30–25	6000	12,000	100±50
25–20	20,000	12,000	330±165
20–16.5	9500	12,000	220±110
16.5–13.5	9500	12,000	260±130

From Hay et al. (1992)

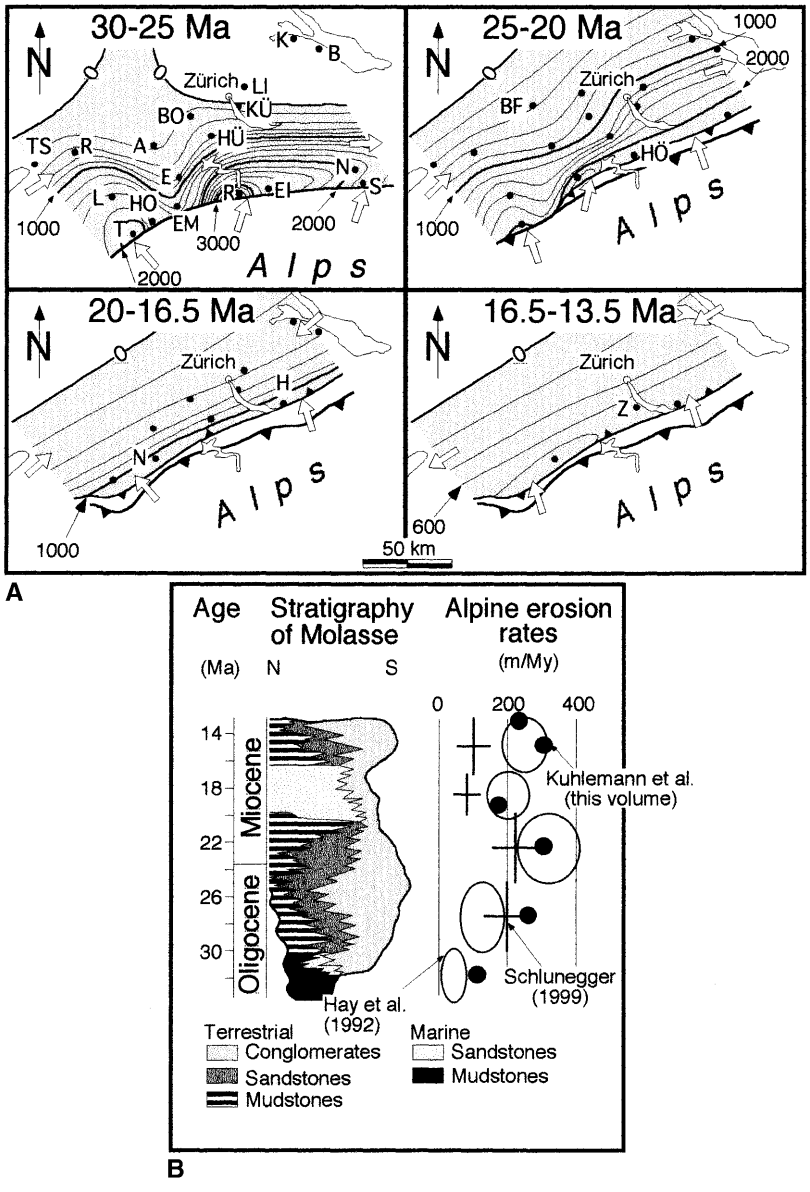

Fig. 4 **A** Isopach maps of the Molasse Basin modified from Schlunegger (1999) complemented with further data from farther east (see Table 1). **B** Average Alpine erosion which that are based on the preserved volume of sediment in the Molasse Basin of central and western Switzerland (Schlunegger 1999) and in the German and Swiss part of the Molasse Basin as well as in sedimentary basins in the north and the south (see legend to Table 3; Hay et al. 1992; Kuhlemann et al. 2000)

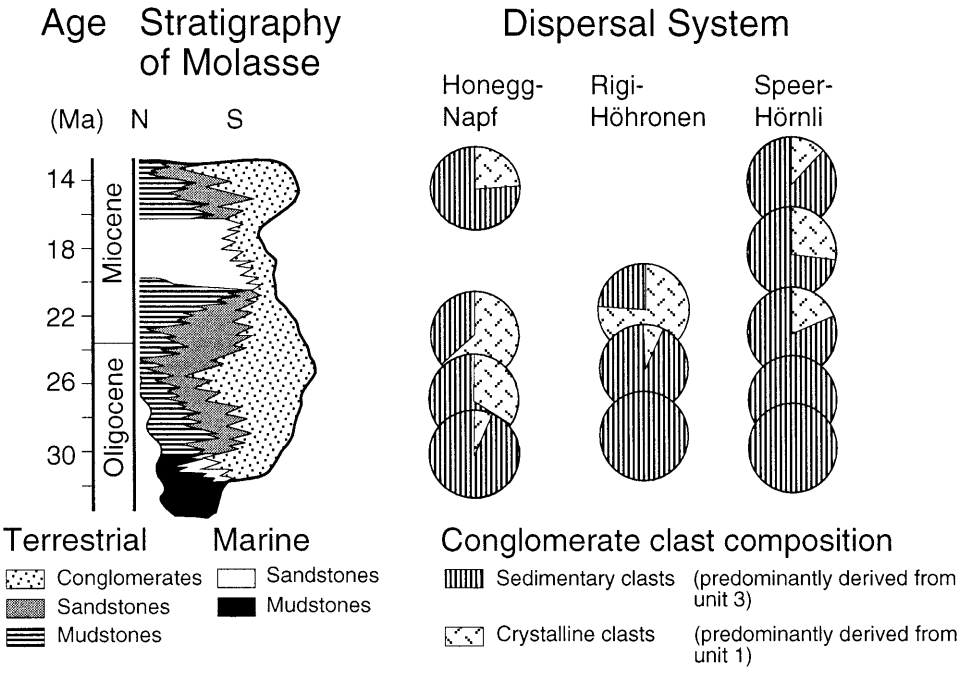

Fig. 5 Petrographic evolution of the Molasse Basin modified after Habicht (1987), Schlunegger et al. (1998), and Kempf et al. (1999). For location of the dispersal systems see Fig. 1

analysis of paleocurrents (Allen et al. 1985) suggest close cells of tidal currents in the Burdigalian seaway with Kelvin waves entering the seaway from the Rhone and Bohemian directions. This implies that the use of 20- to 18-Ma-old preserved volumes of sediment is likely to reflect the actual discharge of sediment to the NAFB. After 18 Ma, and especially during OSM time, the basin was laterally open to the SW (Berger 1992). Therefore, sediment budget analyses for that time interval are likely to represent an underestimate of sediment discharge (e.g., Schlunegger 1999).

Despite differences in the boundary conditions for the mass balance calculations of Hay et al. (1992), Schlunegger (1999), and Kuhlemann et al. (2000), they all reveal similar trends that are characterized by a significant increase of denudation rates of between 150 and 300% during the time period between 30 and 20 Ma (Fig. 4). At ca. 20 Ma surface erosion decreased to rates of between ca. 80 m/My (Schlunegger 1999) and ca. 200 m/My (Hay et al. 1992; Kuhlemann et al. 2000). This implies a ca. 25–40% reduction compared with the previous time interval. Because the NAFB was presumably a closed system between 20 and 18 Ma, the calculation of reduction of sediment discharge of Schlunegger (1999) is likely to be realistic, or might even represent an underestimate. After 16 Ma, average erosion rates started to increase again. Kuhlemann et al. (2000) suggest a significant increase, whereas the data of Schlunegger (1999) and of Hay et al. (1992) imply a slight increase; however, we have to consider that SW-directed sediment export started to occur somewhat after 18 Ma. This implies that the calculations especially of Schlunegger (1999) might represent underestimates.

Erodibilities of Alpine rocks and paleo-exposure of lithotectonic units

A first qualitative analysis of the erosional resistance of the present-day exposed lithologies was presented by Kühni and Pfiffner, (in press). These authors measured the local relief, slopes, and curvatures of the Central Alps using a digital elevation model (DEM) with a horizontal resolution of 250 m. Based on these morphometric parameters, Kühni and Pfiffner (in press) concluded that the three lithotectonic units of the Central Alps presented in Fig. 2 comprise lithologies with contrasting bedrock erodibilities. It is important to note here that Kühni and Pfiffner did not assess specific magnitudes of bedrock erodibilities to Alpine lithologies, they just presented a relative classification into units with very low, low, medium, high, and very high erodibilities. According to these authors, the crystalline rocks of the African and European plates that form unit I (Aar massif, Penninic crystalline rocks; Fig. 2) display low to very low erodibilities. The (meta)sedimentary lithologies of unit 2 (Helvetic and Penninic sedimentary nappes including Bündner Schists and Flysch) are considered to exhibit medium to high erodibilities. The erosional resistance of the carbonates and gneiss/granites which form unit 3 (orgenic lid and Southern Alpine nappes; Fig. 2) appear comparable to those of unit 1. Very high erodibilies are interpreted for the Molasse deposits and the strata of the South Alpine Foreland Basin.

We reconstruct the history of exposure of the three units using the petrographic composition of conglomerates of the NAFB which were deposited by three major dispersal systems (Figs. 1, 5). Certainly, the conglomerate compositions differ in terms of relative abundance of, for example, crystalline clasts, but Fig. 5 reveals that the

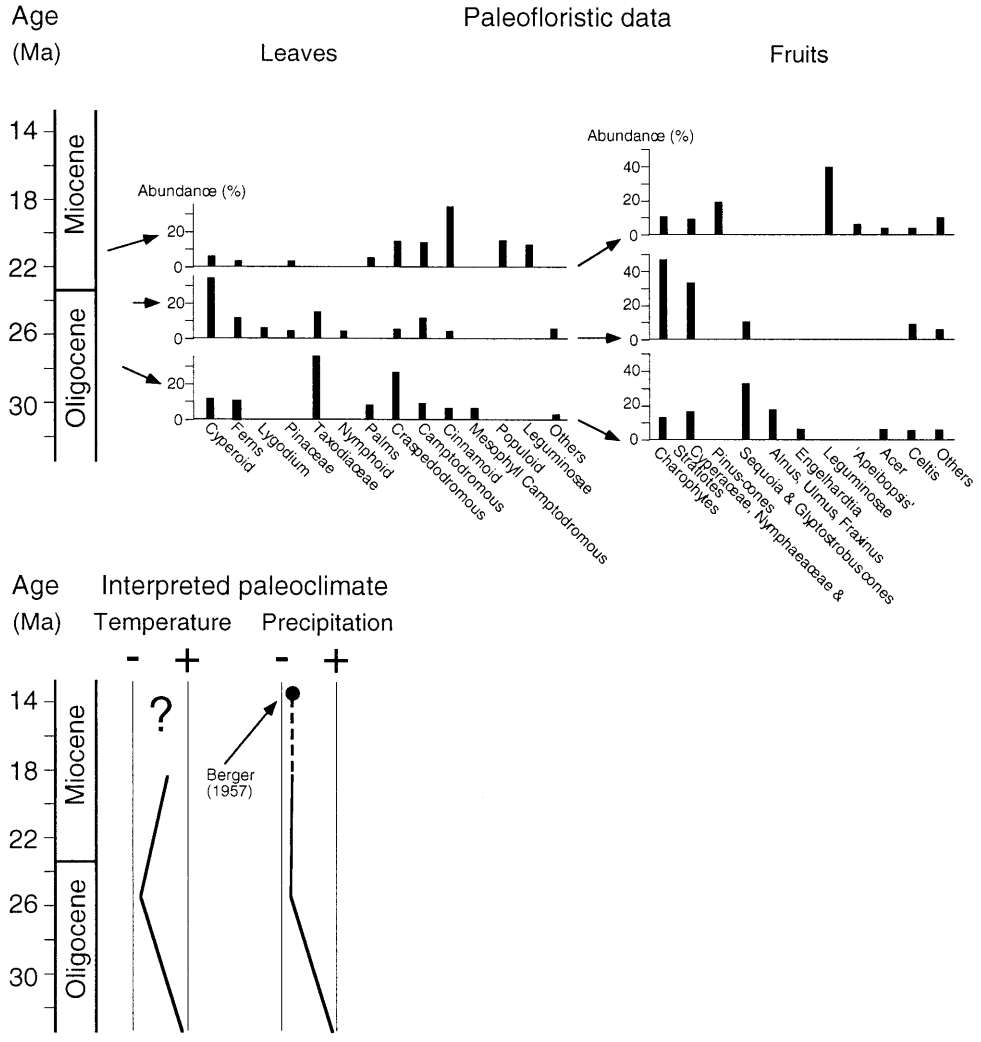

Fig. 6 Palaeofloristic data of western Switzerland for three time slices (27, 25, and 21 Ma) and interpretation of paleoclimate (modified after Berger 1992). The palaeofloristic data for the Middle Miocene (ca. 15 Ma) and the palaeoclimatic interpretation (Berger 1957) is taken from a fossil site located at the German/Swiss border near lake Constance (see Fig. 1)

deposits of these palaeorivers all share the similar petrographic trend that is characterized by (a) erosion of the orogenic lid and Penninic sedimentary nappes in the Late Oligocene (units 3 and 2), and (b) downcutting into the crystalline core of the Alps (unit 1) which was initiated somewhat prior to 20 Ma. It appears that this major shift in the petrographic composition of the foreland basin deposits occurred slightly before the reorganization of the drainage pattern was initiated. Therefore, we interpret that the geometric arrangement of the drainage pattern changed as lithologies with high erosional resistance became exposed (see below). Note that because of the rapid mechanical disintegration of schists (exposed in unit 2; Fig. 2) during transport, they are not represented as clasts in the conglomerates.

Palaeofloristic data and palaeoprecipitation rates

Trends of palaeoclimate for the area surrounding the Central Alps were presented by Berger (1992). This author estimated temporal variations of precipitation rates and palaeotemperature for the NAFB of western Switzerland based on a detailed analysis and discussion of the fossiliferous record of plants. Berger (1992) identified a significant change in the floral assemblage at ca. 25 Ma. This modification is characterized by the disappearance of Palms and Taxads, and the new appearance of Pinaceae, Leguminosae, and Populoids (Fig. 6). Berger interpreted this modification in the floral composition as being due to a change from a humid and hot palaeoclimate, toward a climate with high temperature and low humidity (semiarid conditions; Fig. 6). Warm and presumably semiarid palaeoclimatic conditions have also been interpreted for the North Alpine area of eastern Switzerland during the Middle Miocene. For this area (site Öningen), Berger (1957) identified floral assemblages that are similar to those described for the Early Miocene in western Switzerland (e.g., site Le Locle). However, contemporaneous fossil sites of the SAFB contain abundant leaves from deciduous trees, implying a humid climate for the area surrounding the Southern Alps (Berger 1957). In the region of the Eastern Alps, precipitation rates were presumably constant during the Late Oligocene and the Miocene according to palynologic data (Bruch 1998). It appears, therefore, that the shift

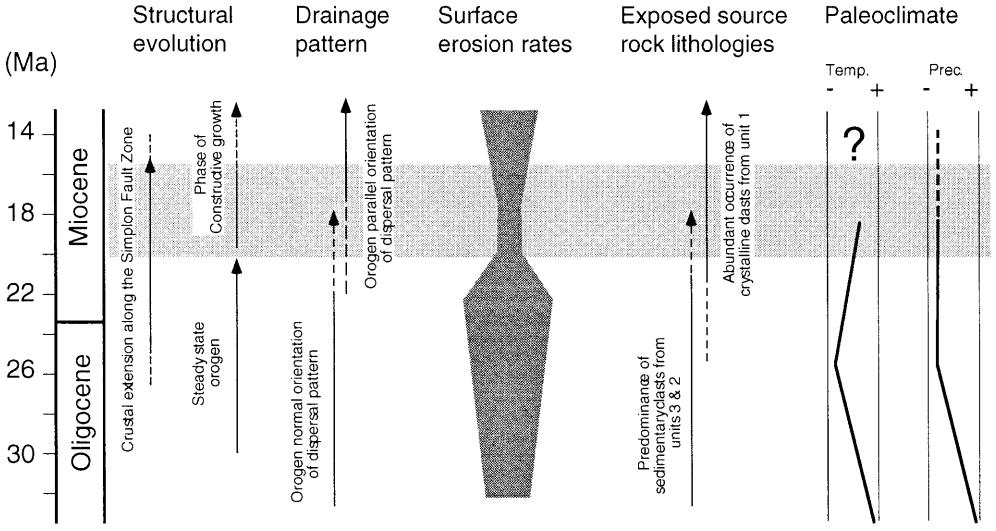

Fig. 7 Chronology of events in the Alpine drainage basin between the Late Oligocene and the Early/Middle Miocene. See text for further discussion

toward drier palaeoclimatic conditions was a local effect that presumably only affected the Alps of Switzerland north of the main drainage divide.

Modeling the topographic evolution of the Central Alps

Kühni and Pfiffner (in press) interpreted that variations in source-rock lithologies exerted a primary control on the erosional history of the Swiss Alps. This interpretation is supported by theoretical models (e.g., Tucker and Slingerland 1996) which assume that fluvial erosion rates are proportional to bedrock erodibility, and that rates of erosion on hillslopes are controlled primarily by rates of channel incision. Nevertheless, because exposure of source-rock lithologies with high erosional resistance does not affect all locations of the Alpine drainage basin at the same time, exhumation and erosion of, for example, the highly metamorphosed core of the Alps (unit 1) influences the erosional mass flux over long, rather than short, time intervals. This is, however, not the case for changes in climate. A climate change must have a short-term measurable impact on the erosional mass flux since variations in precipitation rates usually affect a drainage basin as a whole (e.g., Tucker and Slingerland 1997). Erosion rates may also be affected by other hydroclimatic factors. For example, Tucker and Bras (2000) argued on theoretical grounds that stream erosion and sediment yield should be sensitive to the degree of short-term precipitation variability and to soil hydrologic properties such as infiltration capacity. In some cases, the predicted sensitivity to these controls is greater than the sensitivity to average annual precipitation.

In the following section, we test the potential role of changes in precipitation rates and variations in exposed source-rock lithologies on the history of surface erosion in the Central Alps. Figure 7 represents a summary diagram of the temporal pattern of processes in the Alps. The temporal coincidence between exposure of source rocks with high erosional resistance (unit 1) and reduction of surface erosion rates suggests that exposure of lithologies with enhanced erosional resistance is likely to have affected rates of surface erosion. In this case a reduction of erosion rates may have initiated a phase of surface uplift and a phase of constructive orogen growth (see Schlunegger and Willett 1999). Alternatively, the temporal coincidence between initiation of enhanced rates of crustal extension in the rear of the Alps (slip along the Simplon Fault Zone; Fig. 1) and the climate change suggests that the decrease of precipitation rates might have caused the rear of the wedge to collapse. We use a surface process model to test the combined effect of variations in palaeoclimate and in exposed source-rock lithologies on the change of crustal and topographic growth and the associated erosional mass flux.

As is outlined herein, we model the topographic evolution of the Alps for a single set of input parameters. We are aware that a complete numerical exploration of various possibilities requires a sensitivity test (e.g., Tucker and Slingerland 1997; Kühni and Pfiffner, in press). Our simplified approximation is justified because we only intend to test whether temporal changes in precipiation rates and exposed source rocks can influence the erosional mass flux and the geometric evolution of the Alpine drainage basin. Furthermore, we use the simplest case of tectonic uplift and lithologic architecture with the least contrast between thicknesses and erodibilities (see below). Because we test the simplest scenario of Alpine evolution with the most conservative contrasts of model parameters, our results are also applicable for more complex reconstructions of Alpine evolution.

Erosional processes

Among the various erosional processes discussed in detail by Tucker and Slingerland (1997) and references therein, incisive stream erosion is here considered the most important one because it sets the lower boundary

condition for the adjacent slopes (Whipple and Tucker 1999). Rates of stream incision have been variously considered as proportional to shear stress exerted by the flowing water (e.g., Howard and Kerby 1983; Tucker and Slingerland 1994), total stream power (e.g., Seidl and Dietrich 1992), unit stream power (e.g., Whipple and Tucker 1999), sediment "undercapacity" (e.g., Kooi and Beaumont 1994), or sediment abrasion potential (e.g., Sklar and Dietrich 1998). Although each of these models can produce concave-upward longitudinal stream profiles, we prefer the shear stress approach because of its hydrodynamic basis, its simplicity, and its ability to explain observed stream-profile geometry in tectonically active settings (e.g., Snyder et al. 2000).

According to this model, the rate of change of surface elevation can be described by a combination of local slope (S), drainage area (A) (a surrogate for discharge (Q) where precipitation is uniform over the drainage area), the erosional parameter (K), and crustal uplift rate (U):

$$\frac{\delta h}{\delta t} = U - KS^n A^m \quad (1)$$

For incision proportional to shear stress, various authors have shown that m~1/3 and n~2/3 under the following assumptions: flood flow can be treated as steady and uniform, channel width (W) scales with discharge as $W \sim Q^{0.5}$ (e.g., Leopold and Maddock 1953), and flood discharge scales approximately linearly with drainage area (cf. Slingerland et al. 1993). The erosion parameter, K, lumps together information about rock erodibility, stream channel geometry, mean climate, and precipitation variability (Howard et al. 1994; Whipple and Tucker 1999; Tucker and Bras 2000).

In view of the many uncertainties regarding details of palaeotopography, tectonic history, and palaeoclimate, we adopt this approach as the simplest possible model that still captures the dynamics of a branching fluvial system under variable climate and tectonic forcing. Factors such as glacial erosion, orographic precipitation, and thresholds for fluvial erosion are not considered. Given these simplifications, the value of our modeling lies not in the precise quantitative reconstruction of Alpine topography but rather in demonstrating the feasibility (or lack thereof) of alternative mechanisms to explain the evolution of topography, structure, and drainage patterns during the Late Oligocene and the Early Miocene.

Mass wasting by landsliding is considered to occur where the slope is greater than a threshold value (typically between 20 and 40°). The flux of hillslope erosion due to soil creep and rainsplash depends on the slope gradient. In this case, erosion is generally considered as a diffusive process determined by the topographic curvature (Slingerland et al. 1993):

$$\frac{\delta h}{\delta t} = k\frac{\delta^2 h}{\delta x^2}, \quad k: \text{ lithology and climate dependent diffusion constant.} \quad (2)$$

Magnitudes for the diffusion constant and critical slopes are of second-order importance if (a) the assumption that fluvial incision sets the lower boundary condition for hillslope processes is correct, and (b) the aim is to quantify long-term changes of erosion rates and the resulting erosional mass flux (Allen 1997). Therefore, we tentatively assign values of 30° to critical slopes (Anderson 1994) and 2 m^2/k.y. to the diffusion constant (e.g., Allen 1997). This means that the steepest slopes in the model will be 30°. Below this value, hillslope erosion will be modeled by creep-type hillslope diffusion.

Surface processes model

The model applied in this paper was first described by Slingerland et al. (1993) and was subsequently developed by Tucker and Slingerland (1994, 1996, 1997). It presumes that (a) for long time intervals fluvial incision sets the lower boundary condition for the processes on hillslopes, (b) the shear-stress formula for fluvial erosion (Eq. 1) is adequate to simulate fluvial incision, (c) bedrock erodibility is slope invariant (which is not always the case as suggested by Snyder et al. 2000), and (d) fluvial erosion is scale invariant since erosion rates are an analytical function of slope and discharge. The model uses a fixed rectangular grid which under some conditions can promote a slight anisotropy in simulated drainage patterns. The application of a more flexible mesh is definitely required if the aim is to cope with issues of variable spatial scale and/or dynamic coupling with finite-element mechanical models.

The size of the model of 120×120 km (Fig. 8) is defined by palinspastic reconstructions of the Alps (e.g., Fig. 2; Schmid et al. 1996). We model a time interval of 15 My which encompasses the time span between 30–15 Ma of Alpine evolution. Because we are interested in exploring possible controls on (a) the reduction of surface erosion rates at ca. 20 Ma, and (b) the rearrangement of the drainage pattern that was also initiated at that time, the selected time slice appears appropriate. We use a temporal resolution of 100 years (with smaller time steps used in solution to Eq. (1) as needed), and a spatial resolution of 1 km, which appears to be an adequate balance between computing time and the required resolution of the evolutionary steps. We started from a horizontal plane that is in line with the starting condition of other Alpine model exercises (e.g., Schlunegger and Willett 1999; Kühni and Pfiffner, in press).

Model input parameters

Crustal uplift rates

We use a simple tilt function to simulate crustal uplift of the Central Alps between 30 and 15 Ma (Fig. 8). We assign highest rates of 1 km/My for crustal uplift in the rear of the Alps (backthrusting along the Insubric Line). Also, we assume that the tip of the wedge represented a rotation axis. This simple function simulates the first-or-

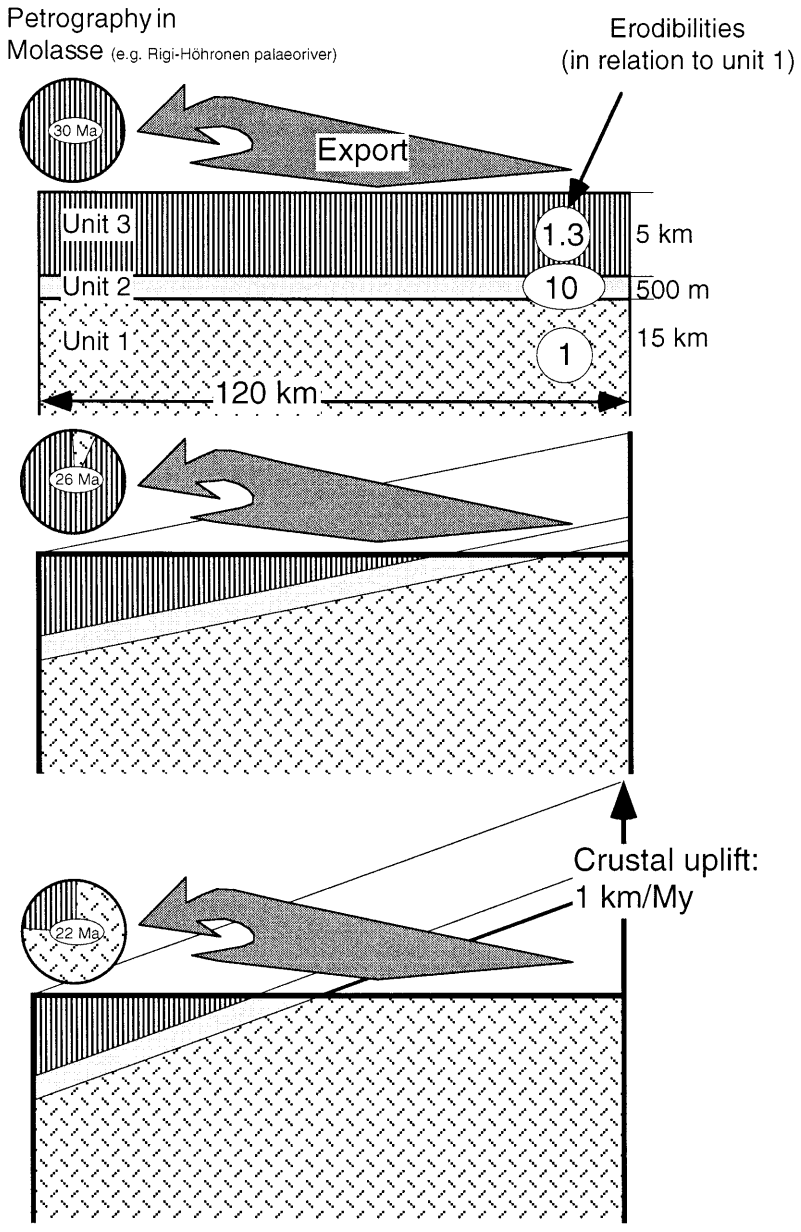

Fig. 8 The configuration of the model. Crustal uplift is modelled as a simple tilt function with maximum rates of uplift in the rear of the wedge (backthrusting along the Insubric Line). The lithologic architecture used in our model is a simplification of the situation of the Alps which is displayed in Fig. 2

der pattern of crustal uplift of the Central Alps between the Late Oligocene and the Early Miocene (e.g., Schmid et al. 1996). We ignore enhanced rates of crustal uplift in the Aar massif (Grindelwald phase of deformation) in our model that started after 20 Ma (Pfiffner et al. 1997) since we intend to test the influence of lithologic differences on the evolution of the Alpine drainage pattern at the simplest tectonic scenario. For simplicity, we do not consider oblique collision between the African and European plates and the resulting westward shift of the location of enhanced rates of crustal uplift along the Insubric Line (Schmid et al. 1996). Finally, we ignore tectonic erosion that occurred by southeastward-directed slip along the Simplon Fault Zone (Fig. 1), because the model cannot consider lateral escape of mass. We justify this simplification because crustal extension in the rear of the wedge is not likely to have significantly modified the large-scale drainage pattern of the Swiss Alps (Eynatten et al. 1999).

Lithologic architecture

We use the simple three-layered model of Fig. 2 to account for the lithologic architecture of the Central Alps. The thicknesses of lithologic units and the associated bedrock erodibilites are displayed in Fig. 8. Besides qualitative studies (Kühni and Pfiffner in press), there are no available data to calibrate bedrock erodibilities for the three lithotectonic units. Magnitudes of bedrock erodibilites for the orogenic lid and the European basement are expected to be limited by the modeled maximum ele-

vations of the mountain belt. However, we do not have any constraints on this parameter. Published reconstructions of the thickness of the Alpine edifice for the Late Oligocene and Early Miocene (e.g., Pfiffner 1986) do not correct elevations for isostatic compensation of the crust.

Theoretical concepts imply that maximum steady-state elevations of a mountain belt depend on rates of crustal uplift, stream power, and bedrock erodibilites (e.g., Whipple et al. 1999). Provided that rates of crustal uplift and bedrock erodibilities are constant, then stream power correlates with the upstream size of the drainage basin that also depends on the cross-sectional width of an orogen. At present, the Swiss Alps are ca. 50–100 km wider than during the Late Oligocene (Schmid et al. 1996), and maximum present-day elevations reach altitudes of ca. 4000 m. Also at present, the area of exposure of bedrock with high erosional resitance is significantly larger than during the Late Oligocene (e.g., Schlunegger et al. 1998). Furthermore, present-day maximum rates of crustal uplift (1.0–1.4 mm/year; Kahle et al. 1997) are comparable to those estimated for the Late Oligocene (Schmid et al. 1996). Accordingly, maximum present-day altitudes of ca. 4000 place upper boundaries for maximum elevations of the Swiss Alps during the Late Oligocene. It can even be speculated that elevations were considerably lower, of the order of between 2500 and 3500 given the 30–50% smaller width of the Oligocene Alps.

The tenfold difference between the erodibility of (meta)sedimentary units (unit 2) and crystalline lithologies (unit 1) as assumed in this paper (Fig. 8) appears a minimum of contrast (e.g., Kühni and Pfiffner, in press). As is shown below, the choice of a minimum of contrasts for the lithologic parameters does not affect the principal results of our model.

Precipitation rates

Several climatic parameters may influence long-term rates of fluvial erosion; these include, in addition to mean annual precipitation, the degree of short-term precipitation variability as well as climatically influenced surface properties, such as infiltration capacity, which influences flood magnitudes (Tucker and Bras 2000). Rather than attempting to reconstruct each of these variables for the geologic past, we simply adopt for experimental purposes a 20% reduction in the climate erosivity factor after 5 My of model run (i.e., at 25 My). As discussed by Tucker and Bras (2000), such a change in climatic erosivity could correspond to changes in any or all of these controlling factors (mean precipitation, variability, and infiltration capacity). The erosivity reduction used in this study can be thought of as corresponding roughly to a twofold decrease in mean annual precipitation accompanied by a modest reduction in soil infiltration capacity (as would be expected under a more arid climate; Tucker and Bras 2000).

Model results

Immediately after initiation of crustal uplift, the modeled orogen evolves toward a distinct geometry with a low- and a high-tapered topography on the pro- and the retro-side of the wedge, respectively (Fig. 9A). A drainage divide develops which is located at ca. 20 km distance from the tip on the retro-side of the orogen. The modeled topography grows continuously until steady-state conditions between the erosional and the crustal mass flux are reached. Topographic growth and the associated increase of surface erosion rates, as well as expansion of the drainage basin, are reflected by the continuous increase of sediment discharge to the north (Fig. 10). At ca. 25 Ma, the model drainage network is completely developed. It is characterized by an orogen-normal direction of dispersion (Fig. 9A). Also at ca. 25 Ma, the modeled topography reaches maximum values of elevation of ca. 2000 m, and the area with maximum local relief between channel and interfluve coincides with the location of the highest curvature of the stream profile, i.e., at x= 30–40 km (Fig. 9A). Maximum values for the local relief are limited by critical values for hillslopes and by the diffusion constant, and by the lateral distance between the trunk streams. Higher values for bedrock erodibilities result in closer distances between the trunk streams, lower elevations of the drainage divide, and shorter response times (Whipple and Tucker 1999).

After 5 Ma of model run (i.e., at 25 Ma), we reduced the erosivity factor by ca. 20% which corresponds to a twofold decrease in mean annual precipitation. As a result, average erosion rates and sediment discharge decrease instantaneously. Because crustal uplift rates were held constant, the model topography starts to grow until steady-state conditions between erosional and lithospheric mass flux are re-established. This appears to be the time when the second peak of sediment discharge is reached, i.e., after 8–9 My of model run, or at ca. 22–21 Ma (Fig. 10).

At ca. 21 Ma (or after 9 My of model run), the (meta)sedimentary rocks of unit 2 and the crystalline core of unit 1 (Fig. 2) become exposed to the surface on the pro-side of the orogen (Fig. 9B). At that time, an orogen-parallel oriented valley develops in the core of the model orogen. Also due to exposure of unit 1, model erosion rates and sediment supply to the pro-side of the orogen decrease, and the orogen starts to grow vertically.

It appears that the presence of a three-layered architecture with a highly erodible unit (unit 2) in the middle is a sufficient condition for the reorganization of the drainage pattern from an orogen-normal to an orogen-parallel orientation of dispersion (Fig. 9C). Similar, perhaps even enhanced, effects on the drainage patterns are expected for higher contrasts of erodibilities and thicknesses between source-rock lithologies. Assignment of highest erosional resistance to unit I is required to simulate a decrease of sediment discharge at ca. 20 Ma (Fig. 10). Other model runs with a constant lithologic architecture do not result in formation of an orogen-paral-

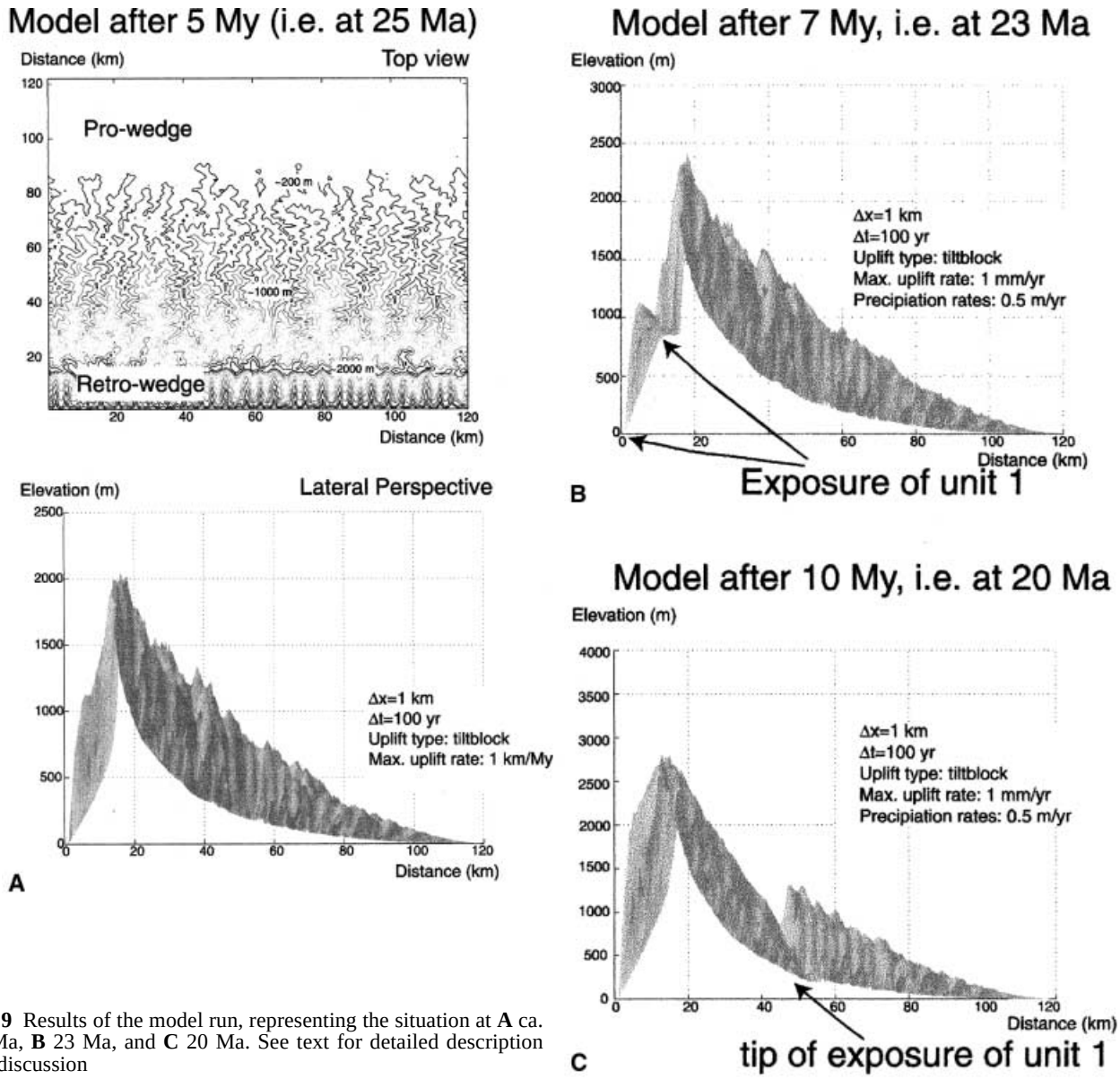

Fig. 9 Results of the model run, representing the situation at **A** ca. 25 Ma, **B** 23 Ma, and **C** 20 Ma. See text for detailed description and discussion

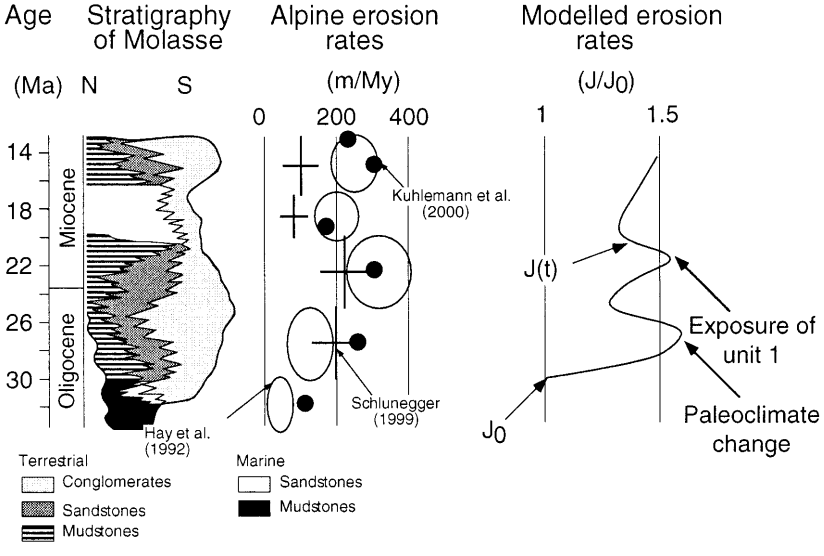

Fig. 10 Comparison of the modelled changes of denudation rates on the pro-side of the Alps with the calculated average erosion rates (Fig. 4). The modelled data is normalized to the situation after 1 My of model run. See text for discussion

lel oriented valley. Even in the case in which domal uplift with rates of 1 mm/year is applied to distal portions on the pro-side of the model orogen (e.g., uplift of the Aar massif), the courses of the rivers are not deflected around the hing of the growing structure (Kühni and Pfiffner, in press). The case of source rocks with low bedrock erodibilities for unit 2 was not explored because this configuration does not apply to the Swiss Alps (Schmid et al. 1996; Kühni and Pfiffner, in press).

Simulations with various scenarios of palaeoclimatic changes result in variations in sediment discharge, but not in a change of the geometric configuration of the drainage basin. It appears that the three-layered architecture of the Alps, and especially the presence of a (meta)sedimentary unit with erodible bedrocks (unit 2) is required to rearrange the configuration of the drainage basin. Also, our study reveals that even in the case of a highly simplified pattern of crustal uplift, the geometry of Alpine dispersion changes when the (meta)sedimentary lithologies become exposed to the surface.

Comparison between model results and geologic data

We were able to successfully reproduce (a) the general trend of sediment discharge to the north (Fig. 10), (b) the petrographic trend of the conglomerates of the foreland basin (Figs. 5, 9), and (c) the change of the drainage pattern from an orogen-normal to an orogen-parallel orientation (Figs. 3, 9).

As outlined previously, the continuous increase in the sediment discharge to the north between the first 5 My of model run appears to reflect (a) the expansion of the drainage basin toward the rear of the wedge, and (b) the continuous vertical growth of the topography until steady-state conditions are reached. Although the resolution of stratigraphic data from the foreland does not really allow identification of an increase in discharge to the basin between 30 and 25 Ma (Fig. 10), the coarsening- and thickening-upward trends of contemporaneous alluvial fan conglomerates which were deposited at enhanced rates of subsidence are likely to reflect an increase of sediment supply rates to the basin (e.g., Kempf et al. 1999). The modeled decrease of sediment discharge at ca. 25 Ma may be reflected by the change from Chattian alluvial fans to Aquitanian lakes and floodplains in the NAFB (Berger 1992).

We successfully modeled the 25–40% decrease of the erosional mass supply to the north at ca. 20 Ma. It appears that this decrease in sediment supply was controlled by modifications of exposed source-rock lithologies. The post-20-Ma continuous increase in the erosional mass supply is also confirmed by the stratigraphic data (Fig. 10) and appears to be controlled by the continuous increase of relief as the topography responds to exposure of rocks with high erosional resistance (Fig. 9).

The model successfully reproduces the petrographic trend of the NAFB characterized by the predominant occurrence of detritus derived from the orogenic lid between 30 and 25 Ma, and increased contribution of detritus from the orogenic core thereafter (Figs. 5, 9). It appears, therefore, that the use of a three-layered lithologic architecture of the Alps combined with a simple tilt-block model for crustal uplift appears to reproduce to first order the exhumation history of the Central Alps. According to the theoretical model, the continuous increase of the relative abundance of detritus derived from the orogenic core appears to be the result of the northward shift of the orogen-parallel oriented drainage system. The trunk stream of this drainage basin changes its position as the tip of unit 2 with high erodiblity moves toward more distal sites.

The model successfully simulates the establishment of a drainage divide in the rear of the wedge, and the change of the northern disperal pattern from an orogen-normal to an orogen-parallel orientation. The latter evolution is caused by the presence of a thin lithologic layer in the Alpine edifice which displays a low resistance to erosion. Kühni and Pfiffner (in press) revealed that the combination of a domal uplift function representing enhanced rates of crustal uplift in the area of the Aar massif (Grindelwald phase of deformation, Fig. 1) with a three-layered model similar to that used in this paper also causes the observed modification of the drainage pattern. In contrast, our model suggests that the use of a more simple scenario is sufficient to explain the development of an orogen-parallel-oriented valley in the interior of the Alps. However, a domal uplift function for the Grindelwald phase of deformation is required to simulate the post-13-Ma northward shift of the main drainage divide (R. Kühni, pers commun.).

Although the first-order characteristics of the evolution of the topography and the erosional mass discharge of the Swiss Alps are successfully imaged by the model, there is a major difference between the model results and the geological data. Tectonic erosion caused by slip along the Simplon Fault Zone which occurred at rates of 0.5–0.8 km/My between 25 and 15 Ma (Grasemann and Mancktelow 1993; Steck and Hunziker 1994; Schlunegger and Willett 1999) is not incorporated in the surface processes model. The influence of crustal extension on modification of the drainage pattern especially in the rear of the Alps is highly controversial. Based on estimates of the rates of change of the exhumation pattern that resulted from tectonic erosion, Schlunegger et al. (1998) argued that slip along the Simplon Fault Zone must have resulted in a northward shift of the major drainage divide of the Central Alps. According to these authors, such a scenario would result in a >25% decrease of the size of the drainage basin on the pro-side of the Alps. Tectonic erosion would also result in a >50% reduction in the contribution of surface erosion to the total amount of exhumation (Schlunegger and Willett 1999). An alternative interpretation of the importance of tectonic erosion on the topographic evolution of the Alps is provided by Eynatten et al. (1999). These authors used the ^{39}Ar–^{40}Ar chronometry applied to detrital mica from

the NAFB. They detected detrital mica with Tertiary cooling ages in post-20-Ma deposits of the NAFB. Eynatten et al. (1999) interpreted the mica ages as revealing close similarities to the thermochronometric data collected from the crystalline core of the Alps which represents the footwall of the Simplon Fault Zone (Steck and Hunziker 1994). Eynatten et al. (1999) concluded that although tectonic erosion is likely to have modified the pattern of exhumation, crustal extension did not significantly change the location of the main drainage divide. It appears, therefore, that ignoring tectonic erosion does not result in significant misinterpretations of the processes that shaped the Oligo/Miocene topography of the Alps.

Implications for Alpine-type evolution

This paper reveals that variations in climate and exposed source-rock lithologies result in a complex pattern of the topographic evolution and the erosional mass flux even if rates of crustal uplift are constant. Indeed, whereas the initial pattern of crustal uplift defines the first-order characteristics of a drainage basin, subsequent modifications of the geometric configuration of the drainage basin can only be achieved if more complexity (e.g., multilayered lithologic architecture) is included in the system. Such complexity might include a highly heterogeneous 3D pattern of tectonic uplift as well as variations in erodibility and palaeoclimate.

The temporal coincidence between commencement of the phase of tectonic erosion in the rear of the Alps and the interpreted shift toward drier climate implies that a change of palaeoclimate is likely to have initiated slip along the Simplon Fault Zone. The modeled reduction of average precipitation rates results in an instantaneous increase of the ratio between crustal uplift rates and surface erosion rates. If the orogen was close to an at-yield mechanical state prior at 25 Ma, which we assume was the case (Schlunegger and Willett 1999), the instantaneous topographic growth might have initiated a phase of lateral escape of mass.

The model suggests that although the palaeoclimate change at 25 Ma presumably caused a phase of enhanced rates of tectonic erosion, it did not initiate the phase of constructive growth. Indeed, even if the decrease of erosion rates was not compensated by tectonic erosion, the Alps would display steady-state conditions between erosional and crustal mass flux at 20 Ma at the latest (Fig. 9). It appears that the distinct lithologic architecture of the Alps characterized by the presence of an orogenic lid with intermediate resistance to erosion, a crystalline core with a low bedrock erodibility, and a thin unit of (meta)sediments with low resistance to erosion in-between (Fig. 8) results in the development of an orogen-parallel-oriented drainage in the center of the orogen that then ultimately results in a phase of crustal growth (Fig. 9). If this situation is established, the Alps start to grow continuously until a critical mechanical state is reached. This appears to be the time when the Southern Alps, and millions of years later the Jura Mountains, were incorporated into the toe of the wedge. In this case, the phase of constructive growth does not necessarily coincide with a modification of the erosional processes. It would instead be the long-term consequence of one or a combination of parameters that control surface erosion.

Acknowledgements This paper was supported by the Deutsche Forschungsgemeinschaft (SCHL 518/1-1). Special thanks go to S. Willett (University of Washington), R. Kühni, and A. Pfiffner (University of Bern), and H. von Eynatten (University of Jena), for stimulating discussions, and to O. Anspach (University of Jena) for technical support. This paper benefited greatly from constructive reviews by P. Allen and J.-P. Berger.

References

Allen PA (1997) Earth surface processes. Blackwell, Oxford

Allen PA, Mange MA, Matter A, Homewood P (1985) Dynamic palaeogeography of the open Burdigalian seaway, Swiss Molasse basin. Eclogae Geol Helv 78:351

Anderson RS (1994) Evolution of the Santa Cruz Mountains, California, through tectonic growth and geomorphic decay. J Geophys Res 99:20161–20179

Berger JP (1992) Paleontologic de la Molasse de Suisse Occidentale, taxonomic, biostratigraphie, paleoecologie, paleogeographie et paleoclimatologie. Habilitation thesis, Univ Fribourg, Fribourg, 405 pp

Berger JP (1996) Cartes paléogéographiques-palinspastiques du bassin molassique suisse (Oligocène inferieur–Miocéne moyen). N Jahrb Geol Paläontol Abh202:1–44

Berger W (1957) Untersuchungen an der obermiozänen (sarmatischen) Flora von Gabbro (Mond Livornesi) in der Toskana, ein Beitrag zur Auswertung tertiärer Blattforen für die Klima- und Florengeschichte. Palaeontogr Ital 51:1–96

Bruch AA (1998) Palynologische Untersuchungen im Oligozän Sloweniens – Paläo-Umwelt und Paleoklima im Ostalpenraum. Tübinger Mikropal Mitt 18:1–193

Eynatten H von, Schlunegger F, Gaupp R, Wijbrans JR (1999) The exhumation of the Lepontine: evidence from $^{40}Ar/^{39}Ar$ laserprobe dating of detrital white micas from the Swiss Molasse Basin. Terra Nova 11:284–289

Gasser U (1968) Die innere Zone der subalpinen Molasse des Entlebuchs (Kt. Luzern), Geologie und Sedimentologie. Eclogae Geol HeIv 61:229–313

Giger M (1991) Geochronologische und petrographische Studien an Geröllen und Sedimenten der Gonfolite Lombarda Gruppe (Südschweiz und Norditalien) und ihr Vergleich mit dem alpinen Hinterland. PhD thesis, Univ Bern, 227 pp

Grasemann B, Mancktelow NS (1993) Two-dimensional thermal modelling of normal faulting; the Simplon fault zone, Central Alps, Switzerland. Tectonophysics 225:155–165

Habicht JKA (1987) Internationales stratigraphisches Lexikon, Band I: Europa, Faszikel 7: Schweiz, Schweizerisches Mittelland. Schweiz Geol Komm, 528 pp

Hay WW, Wold CN, Herzog JM (1992) Preliminary mass-balanced 3D reconstructions of the Alps and surrounding areas during the Miocene. In: Pflug R, Harbaugh JW (eds) Computer graphics in geology, three-dimensional computer graphics in modeling geologic structures and simulating geologic processes. Lecture Notes Earth Sci 41:99–100

Howard AD, Kerby G (1983) Channel changes in badlands. Geol Soc Am Bull 94:739–752

Howard AD, Dietrich WE, Seidl MA (1994) Modeling fluvial erosion on regional to continental scales. J Geophys Res 99: 13971–13987

Kahle HG, Geiger A, Bürki B, Gubler E, Marti U, Wirth B, Rothacher M, Gurtner W, Beutler G, Bauersima I, Pfiffner OA

(1997) Recent crustal movements, geoid and density distribution: contribution from integrated satellite and terrestrial measurements. In: Pfiffner OA, Lehner P, Heitzmann P, Müller S, Steck A (eds) Results of the National Research Program 20 (NRP 20). Birkhäuser, Basel, pp 251–259

Keller B (1989) Fazies und Stratigraphie der Oberen Meeresmolasse (Unteres Miozän) zwischen Napf und Bodensee. PhD thesis, Univ Bern, 277 pp

Kempf O, Matter A (1999) Magnetostratigraphy of the eastern Swiss OSM. Eclogae Geol HeIv 92:97–104

Kempf O, Bolliger T, Kälin D, Engesser B, Matter A (1998) New magnetostratigraphic calibration of Early to Middle Miocene mammal biozones of the North Alpine foreland basin. In: Aguilar JP, Legendre S, Michaux J (eds) Actes du Congrès BiochronM'97. Mém Trav EPHE 2 1, Inst Montpellier, pp 547–561

Kempf O, Matter A, Burbank DW, Mange M (1999) Depositional and structural evolution of a foreland basin margin in a magnetostratigraphic framework: eastern Swiss Molasse Basin. Int J Earth Sci 88:253–275

Kooi H, Beaumont C (1994) Escarpment evolution on high-elevation rifted margins: insights derived from a surface processes model that combines diffusion, advection, and reaction. J Geophys Res 99:12191–12210

Kuhlemann J, Frisch W, Dunkl I, Skékely B (2000) Quantifying tectonic versus erosive denudation by the sediment budget: the Miocene core complexes of the Alps. Tectonophysics 330:1–23

Kühni A, Piffner OA (in press) The geomorphologic fingerprints of the Swiss Alps. Geomorphology

Kühni A, Pfiffner CA (in press) Drainage pattern and tectonic forcing: a model study for the Swiss Alps. Basin Res

Leopold L, Maddock T (1953) The hydraulic geometry of stream channels and some physical implications. Geol Surv Prof Pap 252, 57 pp

Lihou JC, Allen PA (1996) Importance of inherited rift margin structures in the early North Alpine Foreland Basin, Switzerland. Basin Res 8:425–442

Martel AT, Allen PA, Slingerland R (1994) Use of tidal-circulation modeling in paleogeographical studies: an example from the Tertiary of the Alpine perimeter. Geology 22:925–928

Matter A (1964) Sedimentologische Untersuchungen im östlichen Napfgebiet (Entlebuch–Tal der Grossen Fontanne, Kt. Luzern). Eclogae Geol Helv 57:315

Matter A, Homewood P, Caron C, Rigassi D, Van Stujivenberg J, Weidmann M, Winkler W (1980) Flysch and molasse of western and central Switzerland. In: Trümpy R (ed) Geology of Switzerland, a guidebook, Part B, Excursions. Schweiz Geol Komm, pp 261–293

Pfiffner OA (1986) Evolution of the north Alpine foreland basin in the Central Alps. In: Allen PA, Homewood P (eds) Foreland basins. Int Assoc Sediment Spec Publ 8:219–229

Pfiffner OA, Sahli S, Stäuble M (1997) Structure and evolution of the external basement uplifts. In: Pfiffner OA, Lehner P, Heitzmann P, Müller S, Steck A (eds) Results of the National Research Program 20 (NRP 20). Birkhäuser, Basel, pp 139–153

Platt NH, Keller B (1992) Distal alluvial deposits in a foreland basin setting: the Lower Freshwater Molasse (Lower Miocene), Switzerland: sedimentology, architecture and palaeosols. Sedimentology 39:545–565

Schlunegger F (1999) Controls of surface erosion on the evolution of the Alps: constraints from the stratigraphies of the adjacent foreland basins. Int J Earth Sci 88:285–304

Schlunegger F, Willett SD (1999) Spatial and temporal variations in exhumation of the central Swiss Alps and implications for exhumation mechanisms. Geol Soc Lond Spec Publ 154:157–179

Schlunegger F, Slingerland R, Matter A (1998) Crustal thickening and crustal extension as controls on the evolution of the drainage network of the central Swiss Alps between 30 Ma and the present: constraints from the stratigraphy of the North Alpine Foreland Basin and the structural evolution of the Alps. Basin Res 10:197–212

Schmid SM, Pfiffner OA, Froitzheim N, Schönborn G, Kissling E (1996) Geophysical–geological transect and tectonic evolution of the Swiss-Italian Alps. Tectonics 15:1036–1064

Seidl MA, Dietrich WE (1992) The problem of channel erosion into bedrock. Catena Suppl 23:101–124

Sinclair HD, Allen PA (1992) Vertical versus horizontal motions in the Alpine orogenic wedge: stratigraphic response in the foreland basin. Basin Res 4:215–232

Sklar L, Dietrich WE (1998) River longitudinal profiles and bedrock incision models: stream power and the influence of sediment supply. In: Tinkler KJ, Wohl EE (eds) Rivers over rock, fluvial processes in bedrock channels. Geophys Monogr 107:237–260

Slingerland R, Harbaugh J, Furlong K (1993) Simulating clastic sedimentary basins. Prentice-Hall, Englewood Cliffs, New Jersey

Snyder NP, Whipple KX, Tucker GE, Merritts D (2000) Landscape response to tectonic forcing; DEM analysis of stream profiles in the Mendocino Triple Junction region, northern California. Geol Soc Am Bull 112:1250–1263

Steck A, Hunziker J (1994) The Tertiary structural and thermal evolution of the Central Alps: compressional and extensional structures in an orogenic belt. Tectonophysics 238:229–254

Stürm B (1973) Die Rigischüttung. Sedimentpetrographie, Sedimentologie, Paläogeographic, Tektonik. PhD thesis, Univ Zürich, 98 pp

Tucker GE, Bras RL (1998) Hillslope processes, drainage density, and landscape morphology. Water Resour Res 34:2751–2764

Tucker GE, Bras RL (2000) A stochastic approach to modeling the role of rainfall variability in drainage basin evolution. Water Resour Res 36:1953–1964

Tucker GF, Slingerland R (1994) Erosional dynamics, flexural isostacy, and long-lived escarpments: a numerical modeling study. J Geophys Res 99:12229–12244

Tucker GE, Slingerland R (1996) Predicting sediment flux from fold and thrust belts. Basin Res 8:329–349

Tucker GE, Slingerland R (1997) Drainage basin response to climate change. Water Resour Res 33:2031–2047

Whipple KX, Tucker GE (1999) Dynamics of the stream power river incision model: implications for height limits of mountain ranges, landscape response timescales and research needs. J Geophys Res 104:17661–17674

Whipple KX, Kirby I, Brocklehurst SH (1999) Geomorphic limits to climate induced increases in topographic relief. Nature 401:39–43